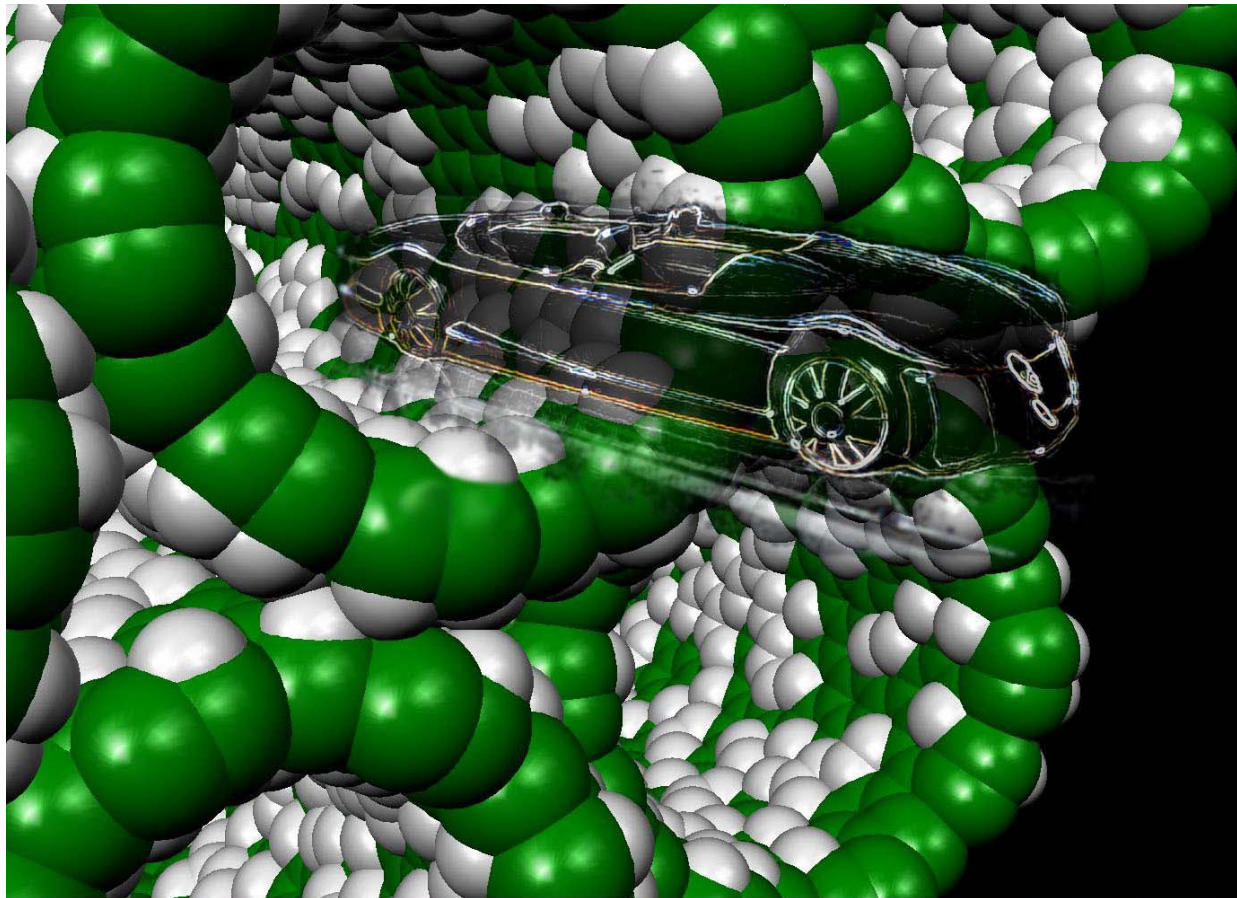


Hydrogenation of Single Walled Carbon Nanotubes

Anders Nilsson

Stanford Synchrotron Radiation Laboratory (SSRL) and Stockholm University



Coworkers and Acknowledgement

A. Nikitin¹⁾, H. Ogasawara¹⁾, D. Mann²⁾, Z. Zhang³⁾, X. Li³⁾, H. Dai²⁾, KJ Cho³⁾

1) Stanford Synchrotron Radiation Laboratory

2) Department of Chemistry, Stanford University

3) Department of Mechanical Engineering, Stanford University

Physical Review Letters 95, 225507 (November 2005)

Highlights:

http://www-ssrl.slac.stanford.edu/research/highlights_archive/swcn.html

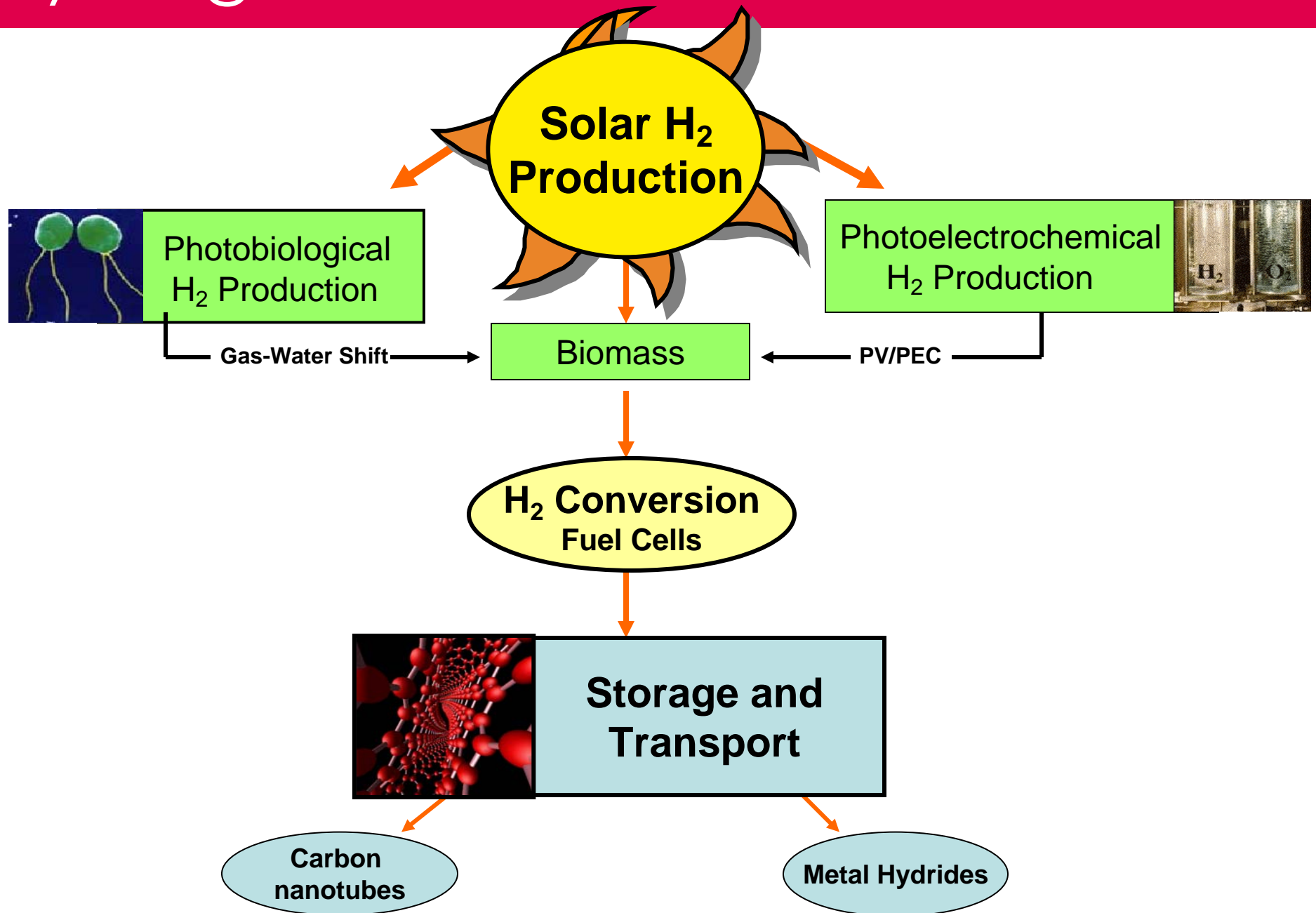
http://www-als.lbl.gov/als/science/sci_archive/129nanotube.html

FUNDING:



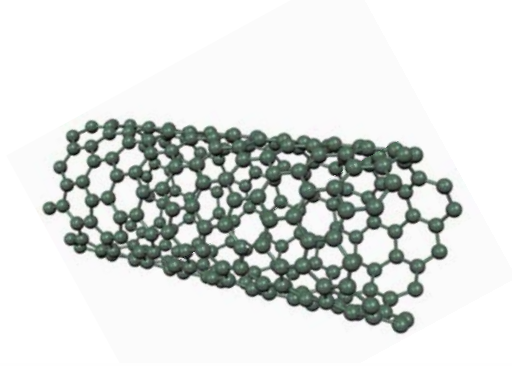
Global Climate & Energy Project
STANFORD UNIVERSITY

Hydrogen Dream

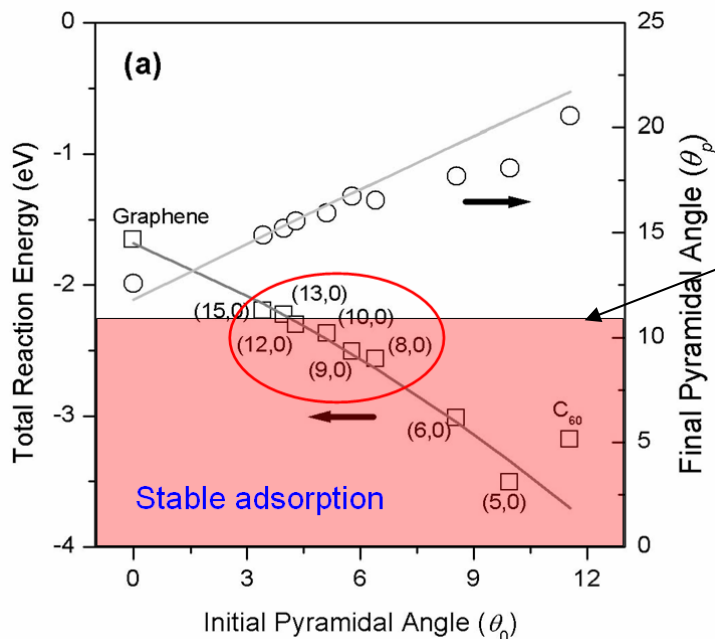
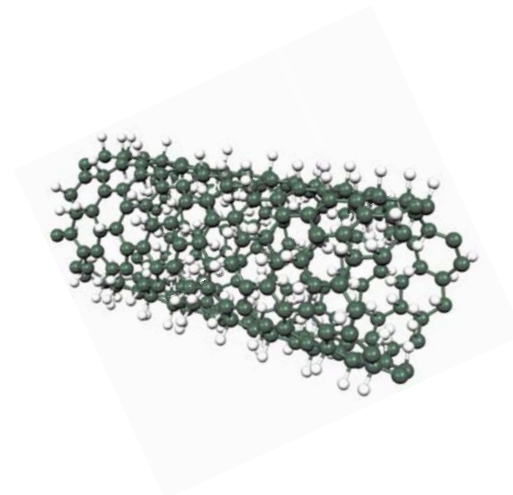


Chemisorption of H atoms on Carbon Nanotubes

Idea: to store hydrogen in the chemisorbed form on the nanotube surface



hydrogenation

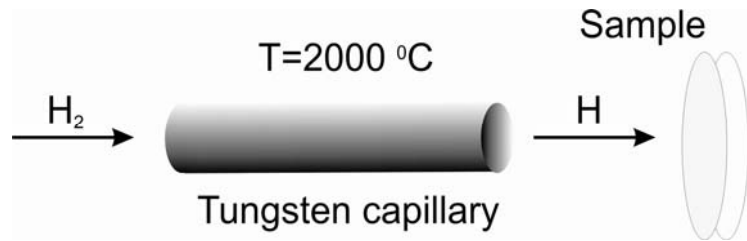


H-H bond energy 4.5 eV

Adsorption Energy Decreases with diameter

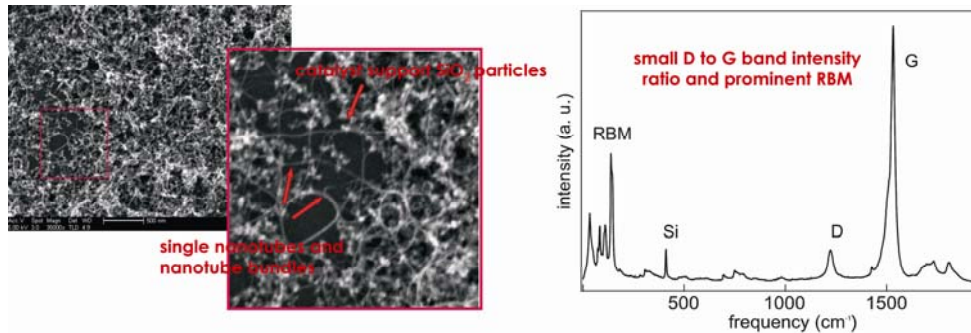
Investigation strategy

Hydrogenation: *in situ* atomic hydrogen treatment



- elimination of H₂ dissociation step from hydrogenation process
- well controlled environment (base pressure < 1 10⁻⁹ Torr)

Samples: "as grown" CVD SWCN films



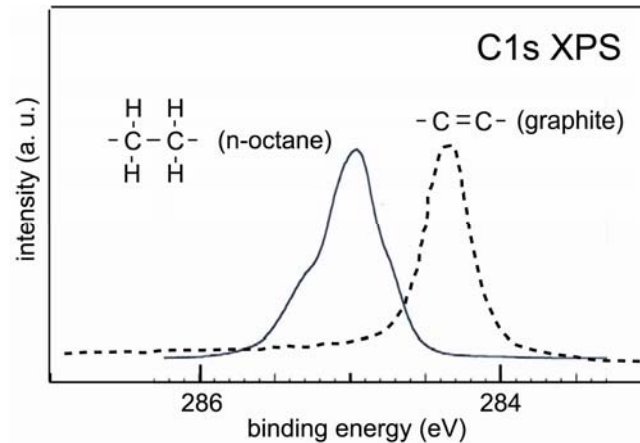
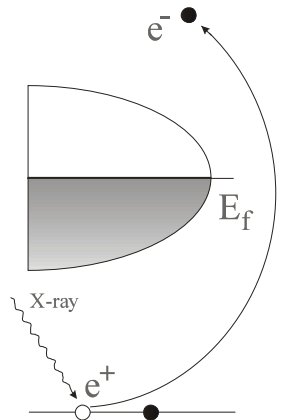
- low defect / amorphous carbon concentration (small D to G band intensity ratio)
- low concentration of contamination (*in situ* annealing up to 900 C)

Probing tools: X-ray photoelectron spectroscopy (XPS) and X-ray adsorption spectroscopy (XAS)

- XPS and XAS allow to observe the formation of C-H bonds through the modification of the carbon nanotube electronic structure around specific carbon atoms

Probing tools

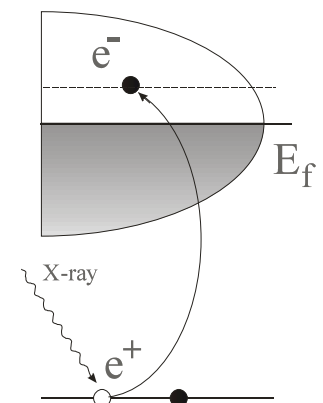
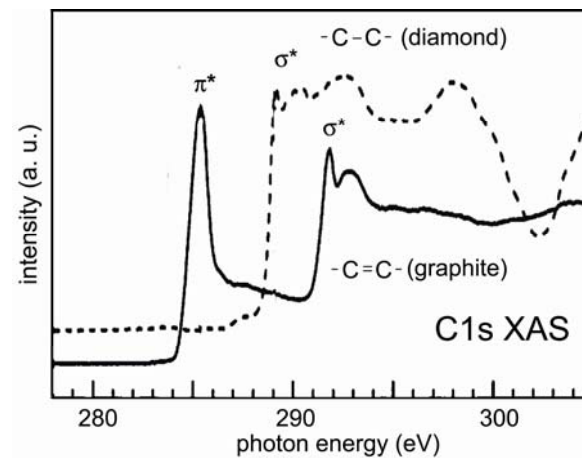
X-ray photoelectron spectroscopy (XPS)



C1s XPS spectra of n-octane and graphite (Weiss et al., 2003, Bennich et al., 1999)

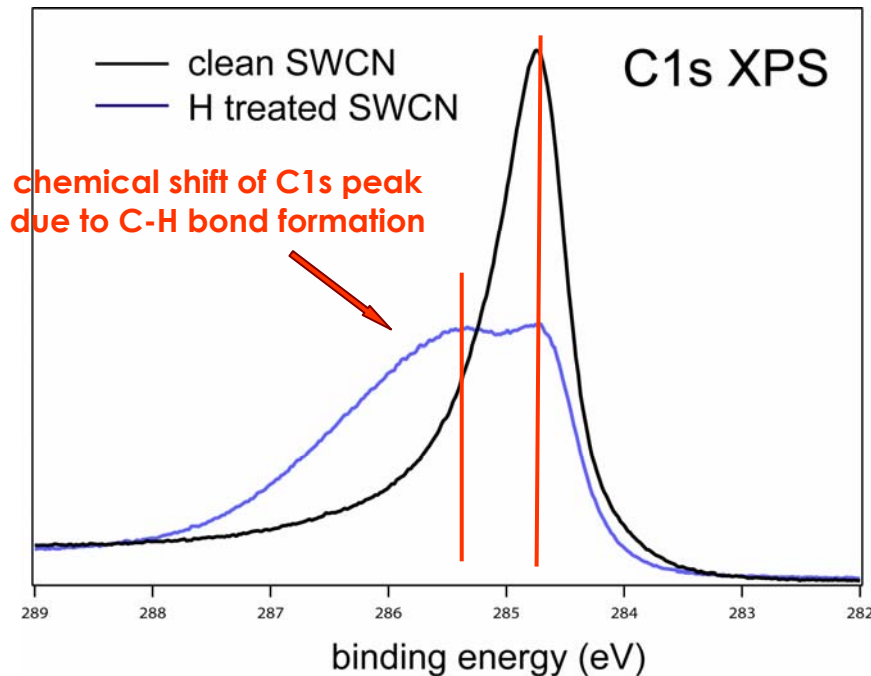
X-ray absorption spectroscopy (XAS)

Carbon K-edge XAS spectra of graphite and diamond (Garo et al., 2001)



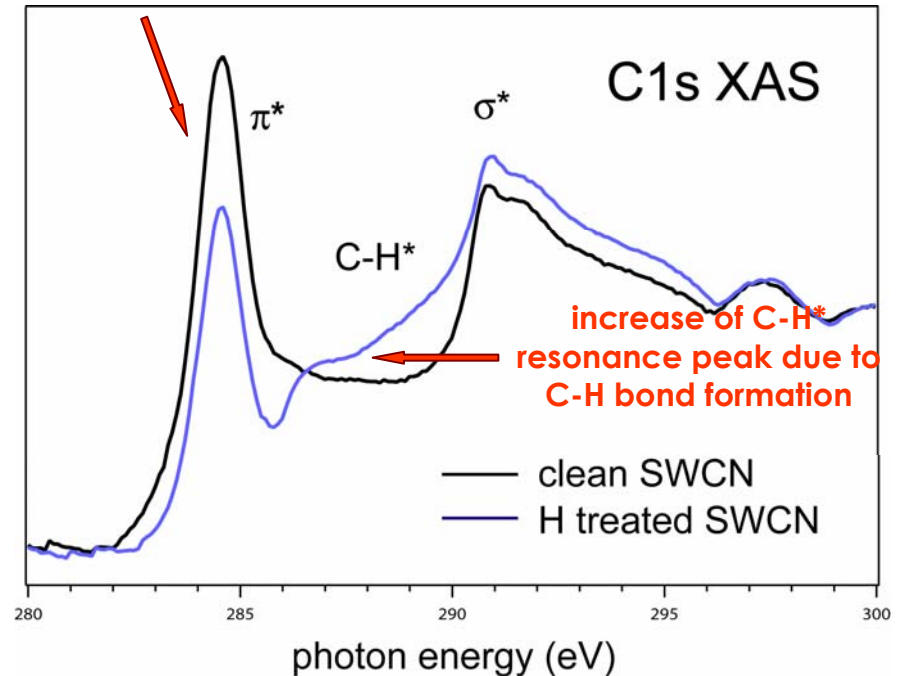
Hydrogenation induced changes in XAS and XPS spectra

C1s XPS spectra of the clean and hydrogenated SWCN films



Carbon K-edge XAS spectra of clean and hydrogenated SWCN films

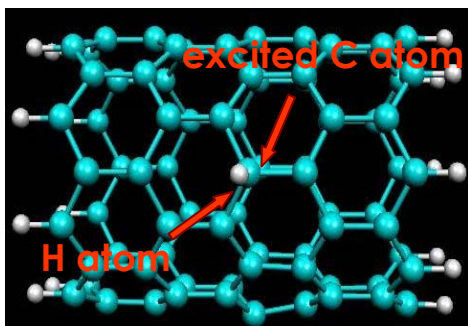
decrease of π^* resonance peak due to C-H bond formation



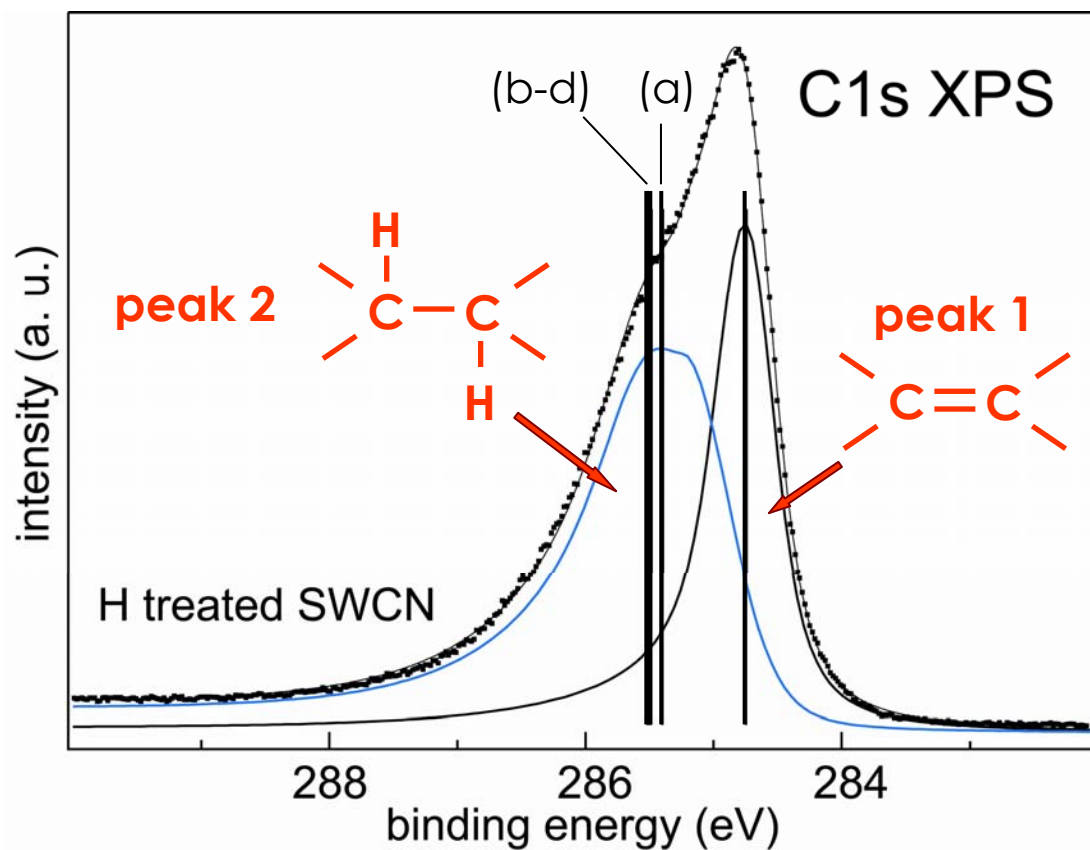
The hydrogenation degree determination from XPS spectra

Calculated C1s chemical shift values (MD and DFT)

(n,m)	D, nm	Shift, eV
(a) (10,0)	0.78	0.65
(b) (12,0)	0.94	0.77
(c) (15,0)	1.16	0.74
(d) (22,0)	1.72	0.76



Decomposition of C1s XPS for hydrogenated SWCN film



$$\text{Hydrogenation} = I_{\text{peak 2}} / (I_{\text{peak 1}} + I_{\text{peak 2}}) * 100 \text{ at } \%$$

Samples

"as grown" chemical vapor deposition (CVD) SWCN films

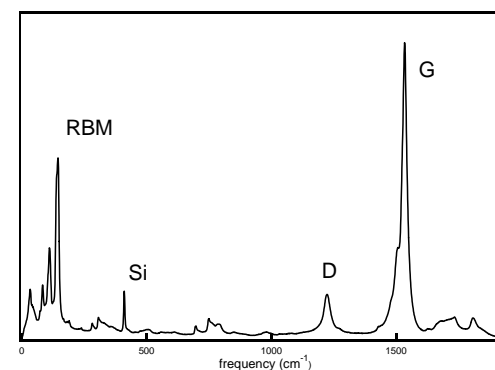
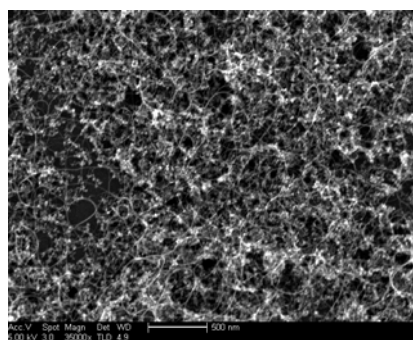
Growth condition

SEM picture

Raman spectra

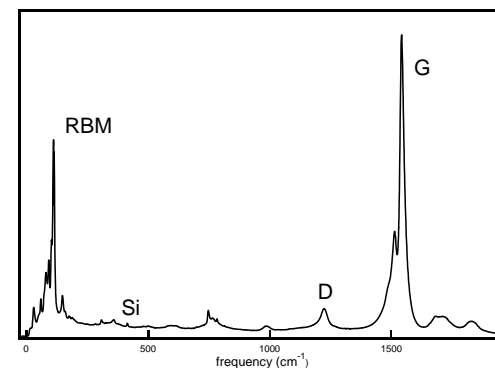
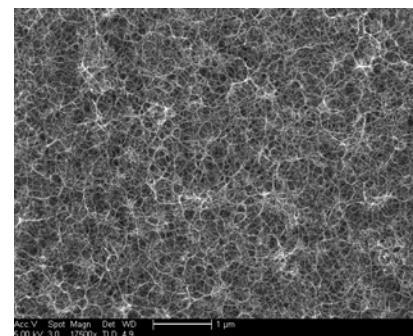
Type 1

Catalyst: FeCo on SiO₂
Gas: 400 sccm CH₄, 70 sccm H₂
Temperature: 850 C



Type 2

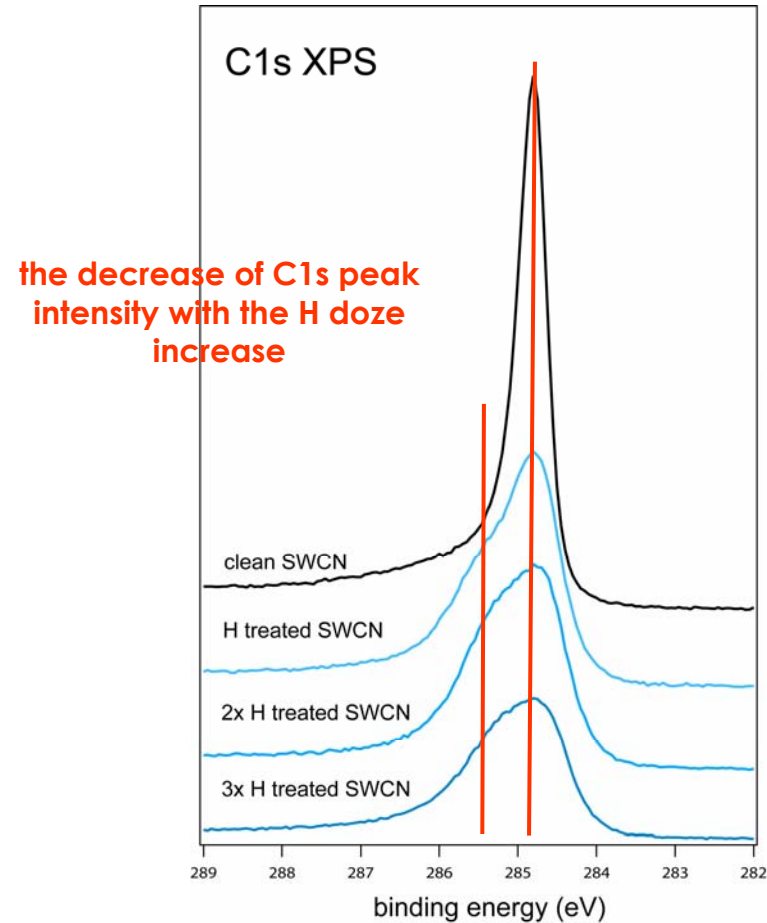
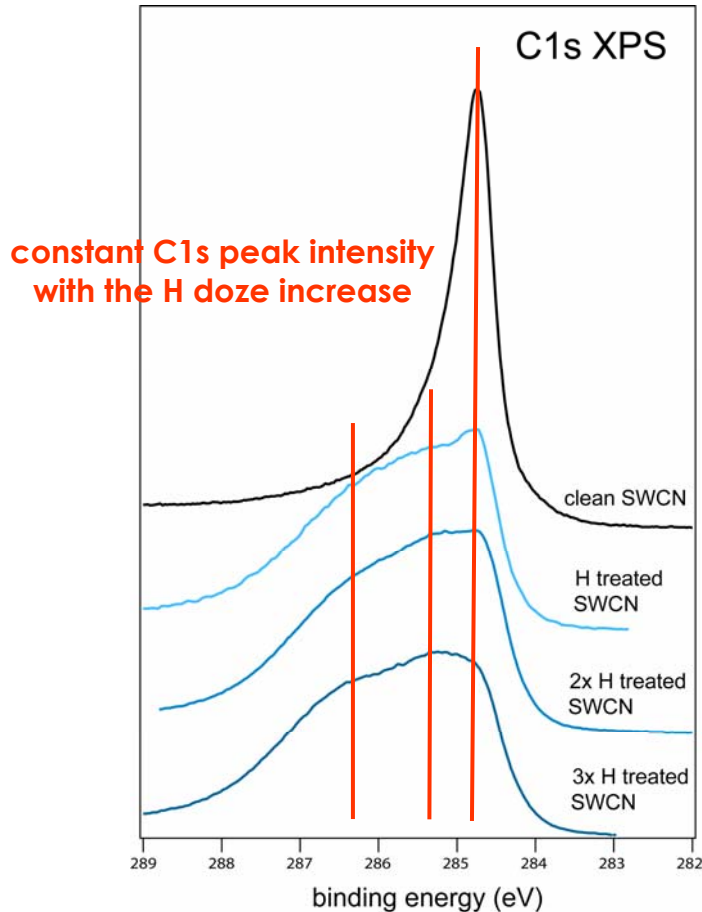
Catalyst: FeCoMo on SiO₂
Gas: 300 sccm EtOH, 300 sccm Ar
Temperature: 850 C



- prominent RBM band - relatively narrow SWCN diameter distribution
- small D to G band intensity ratio - low defect/ amorphous carbon concentration
- most of SWCN are in the bundles

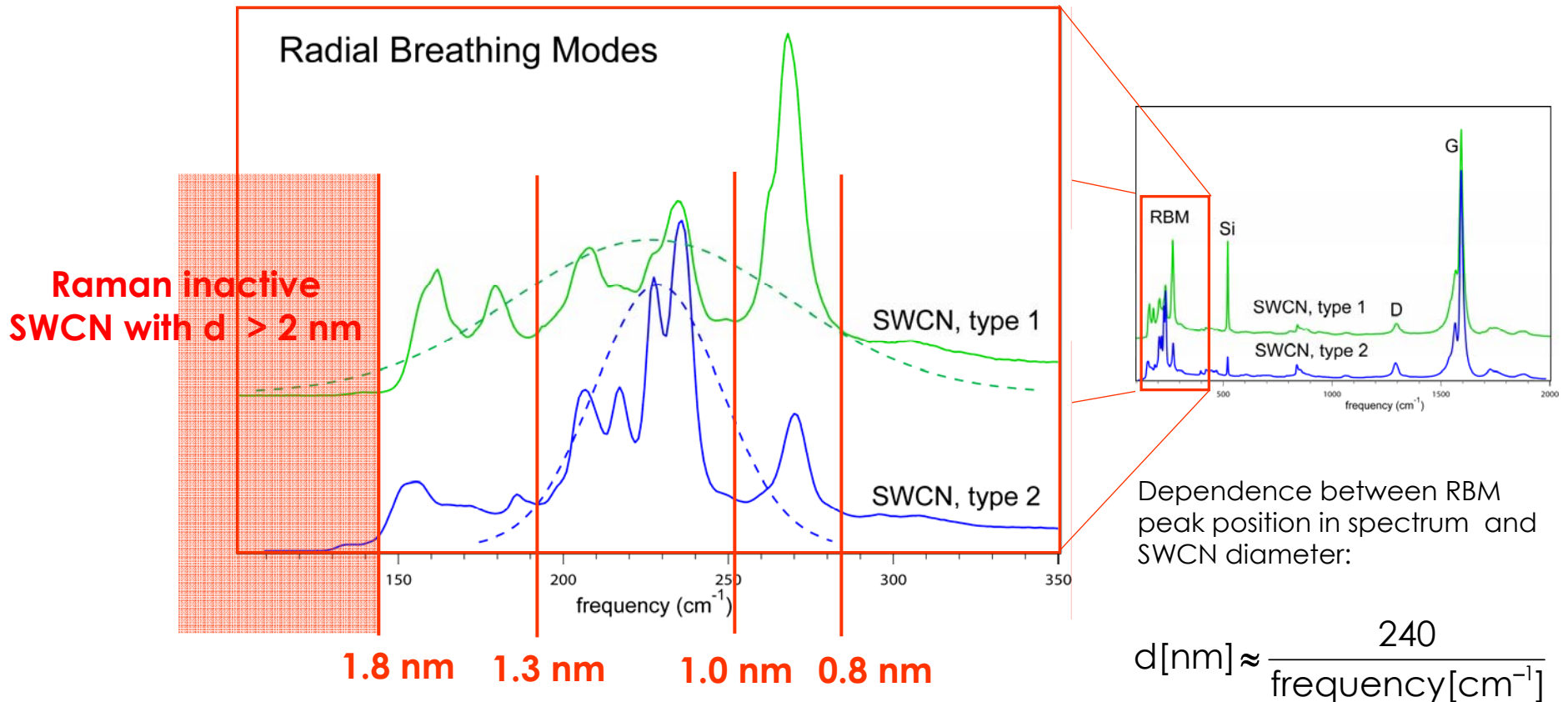
The influence of SWCN diameter on hydrogenation process

Hydrogenation sequence of SWCN, type 1 Hydrogenation sequence of SWCN, type 2



For the SWCN, type 2 under H treatment **etching of the material** starts before reaching high degree of hydrogenation in comparison with SWCN, type 1

The influence of SWCN diameter on hydrogenation process

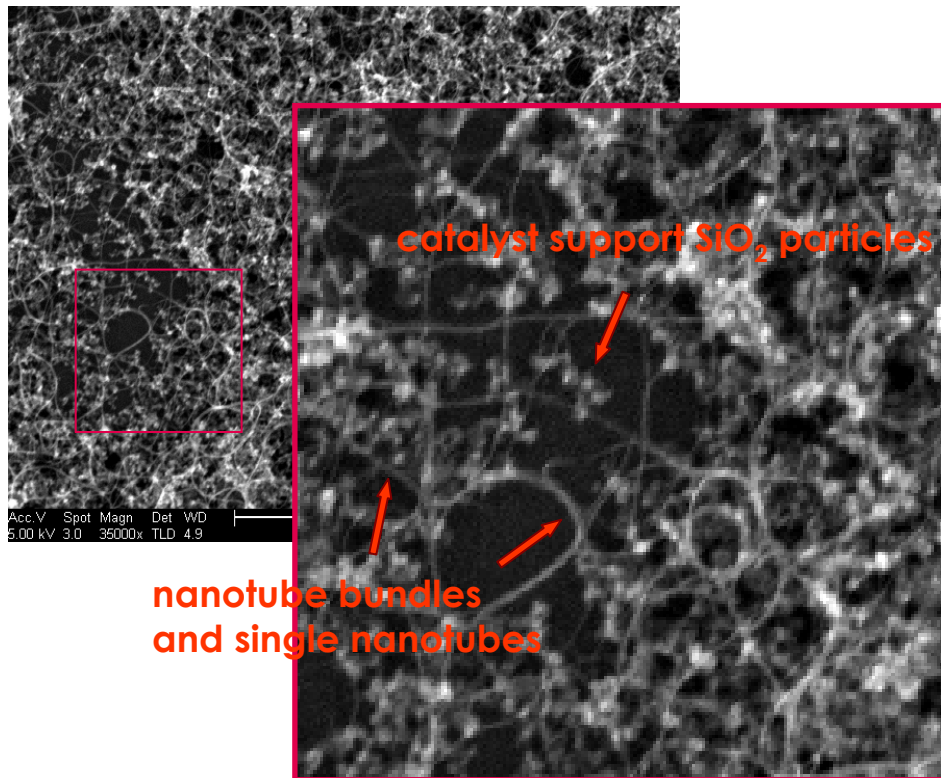


- theoretical prediction of H induced "unzipping" for the small ($d < 1.2$ nm) SWCN (Lu et al PRB 68, 205416)
- experimentally observed selective H^+ plasma etching for different types of SWCN (Zhang et al JACS 2006, 128, 6026)

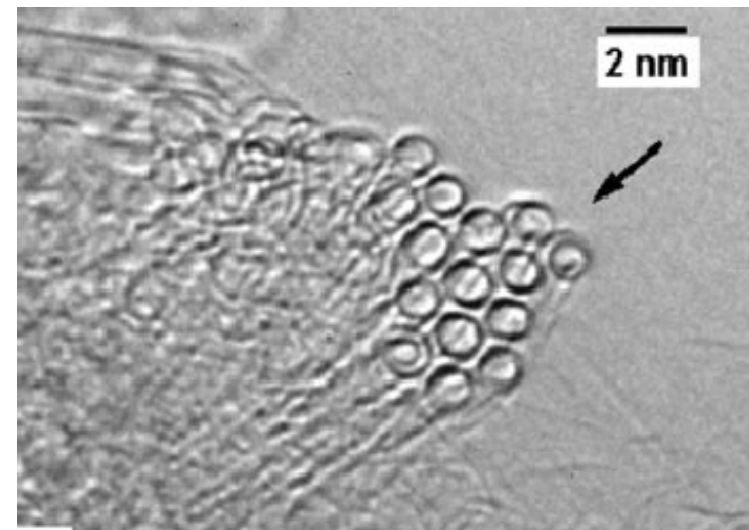
For SWCN with **different diameters** H induced etching of the material starts at **different degree of hydrogenation**

The morphology of SWCN film

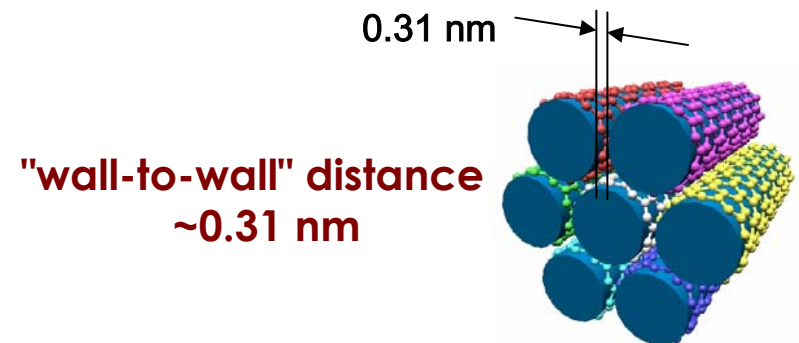
SEM picture of studied film



TEM picture of SWCN bundle



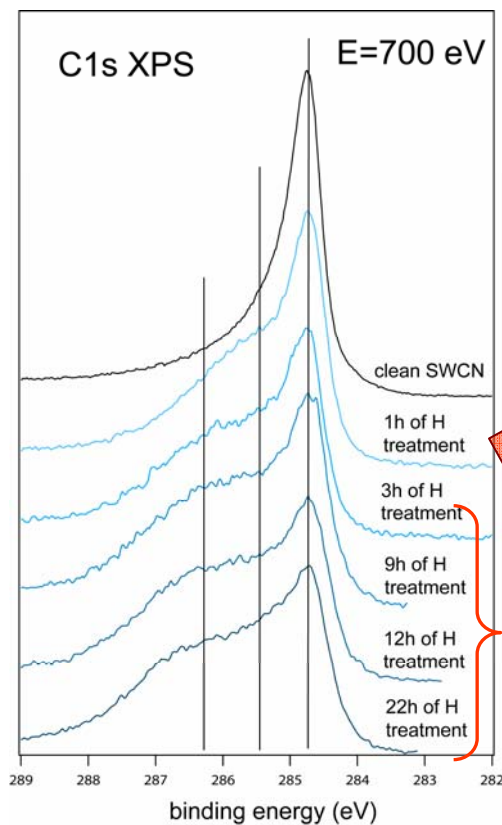
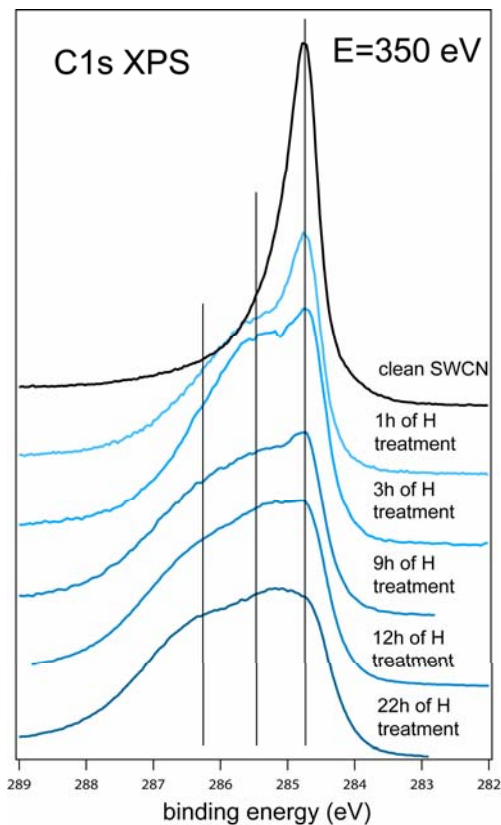
(Terrones et al Science 228, 1226)



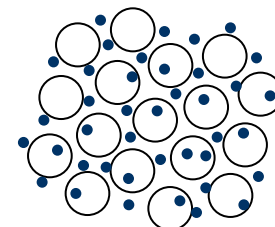
How does bundling morphology influence on hydrogenation ?

The hydrogenation depth of SWCN film

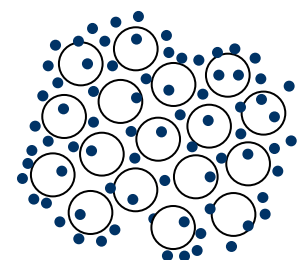
Hydrogenation sequence for SWCN, type 1 measured at different excitation energies



uniform hydrogenation of SWCN bundle up to ~50 -60 %



Increase of hydrogenation degree only on the SWCN bundle surface at additional H treatment

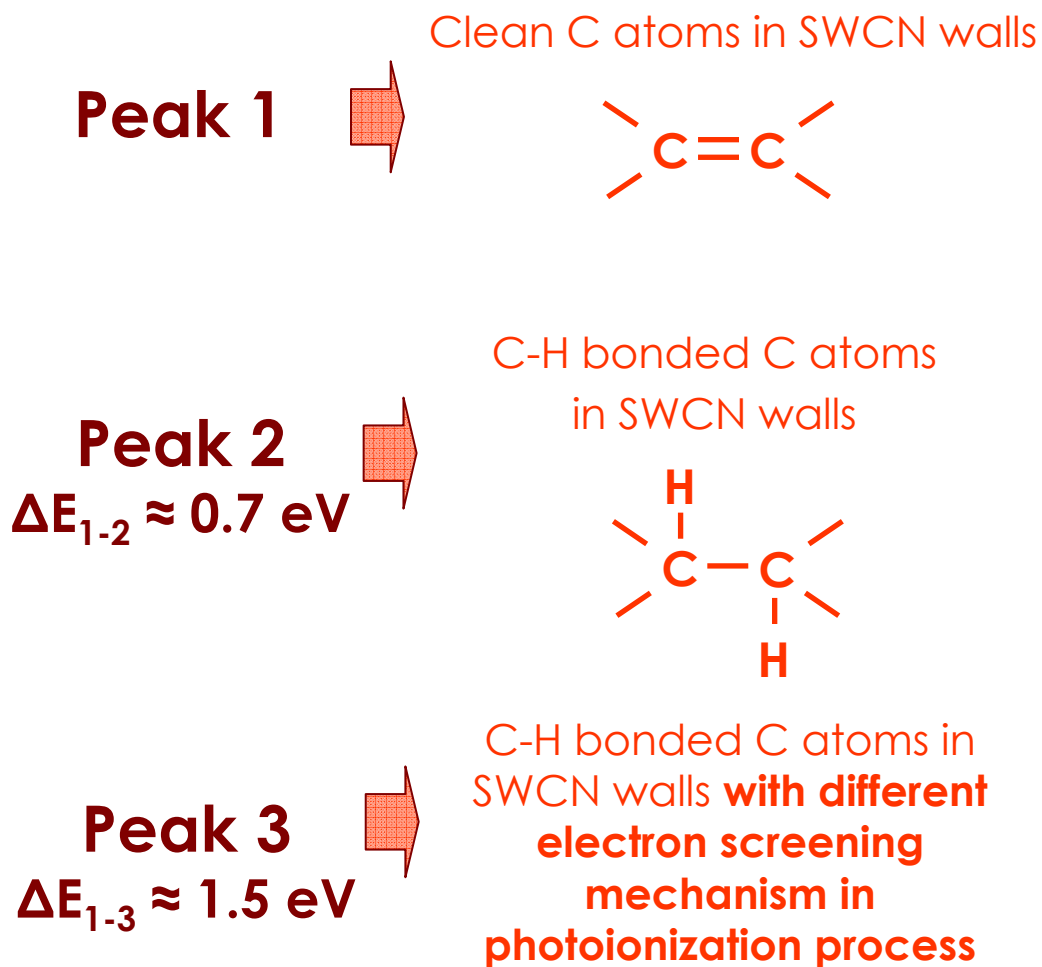


$E_{hu} = 350 \text{ eV}$ ($E_{kinC1s} = 65 \text{ eV}$)
 $\lambda \approx 0.3 \text{ nm}$ (more surface sensitive)

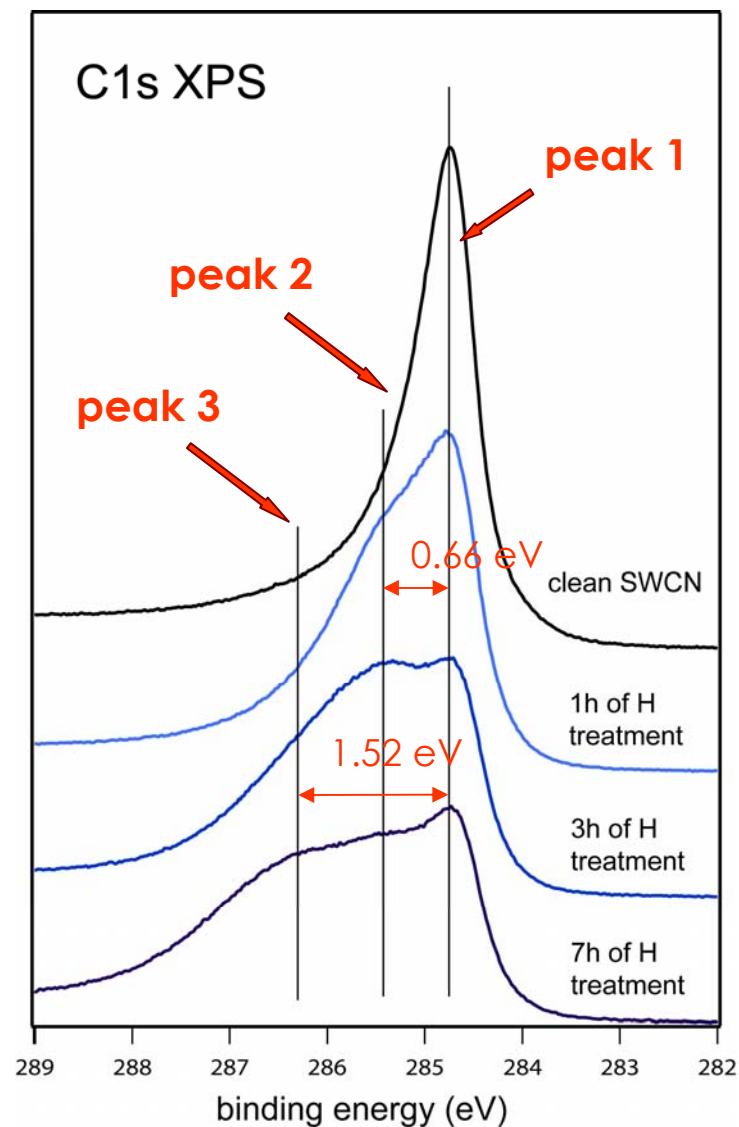
$E_{hu} = 700 \text{ eV}$ ($E_{kinC1s} = 415 \text{ eV}$)
 $\lambda \approx 1 \text{ nm}$ (more bulk sensitive)

Hydrogenation is **not uniform** across the SWCN bundle

Structure of XPS C1s spectrum for highly hydrogenated SWCN

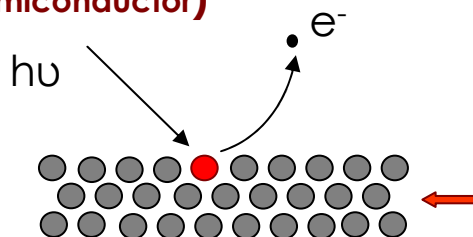


Hydrogenation sequence of SWCN, type 1



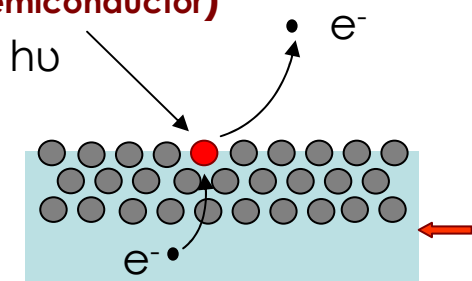
The electron screening in photoionization process

Atom photoionization in the system without delocalized electrons (insulator or wide bandgap semiconductor)



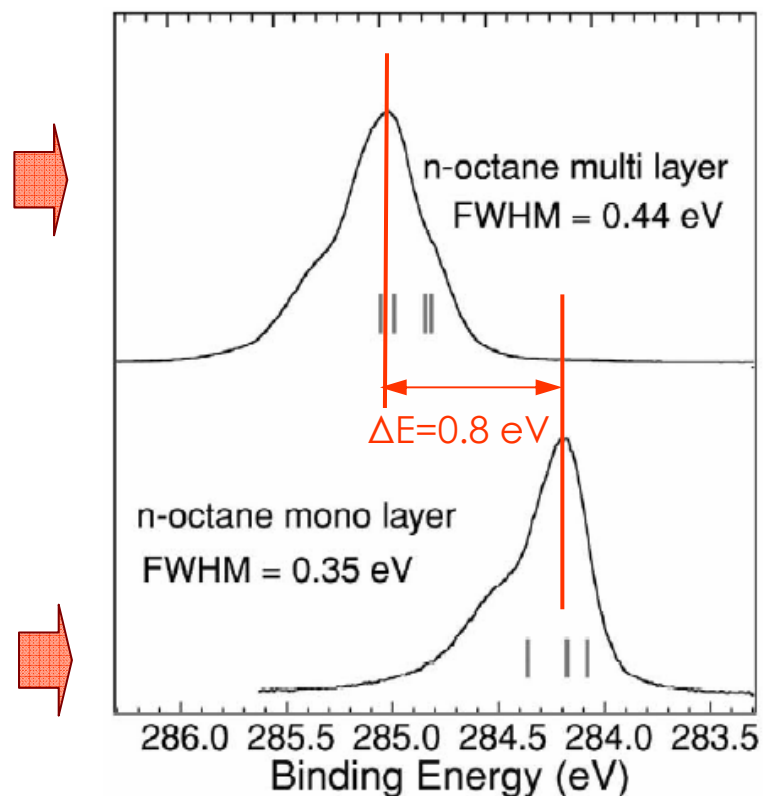
No delocalized electrons in the system

Atom photoionization in the system with delocalized electrons (metal or narrow bandgap semiconductor)



Delocalized electrons in conduction band

The transfer of delocalized electron to the ionized atom changes the final state

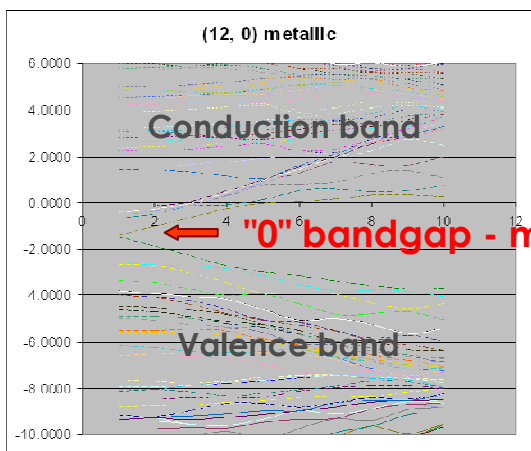


C1s XPS spectra of monolayer of n-octane on Cu substrate and n-octane multilayer (Weiss et al., 2003, J. of Elect. Spectr. 2003, 128, 129)

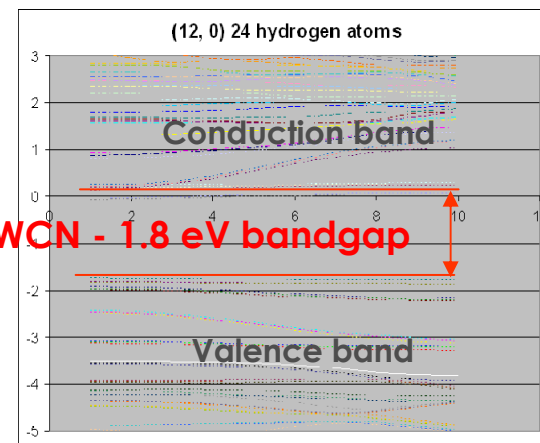
The presence of delocalized electrons in the system leads to the **different final state** in the photoionization process and **peak shift** in the XPS spectrum

The electron screening in hydrogenated SWCN

Hydrogenation induced band gap increase in SWCN

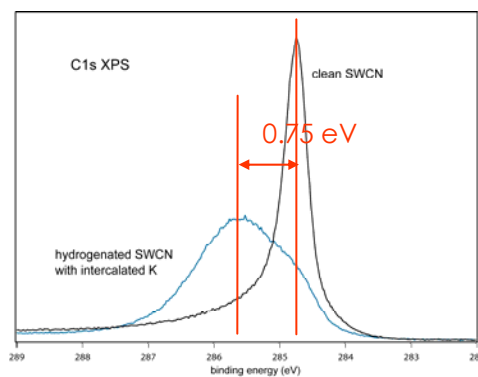
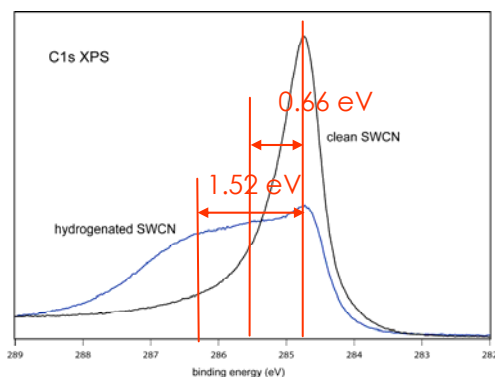


Calculated DOS of clean (12,0) SWCN



Calculated DOS of hydrogenated (12,0) SWCN

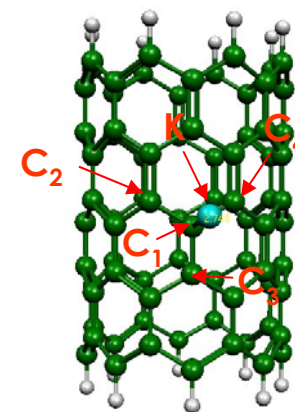
Hydrogenated SWCN with intercalated K



C1s XPS spectra of hydrogenated SWCN with (right) and without (left) intercalated K

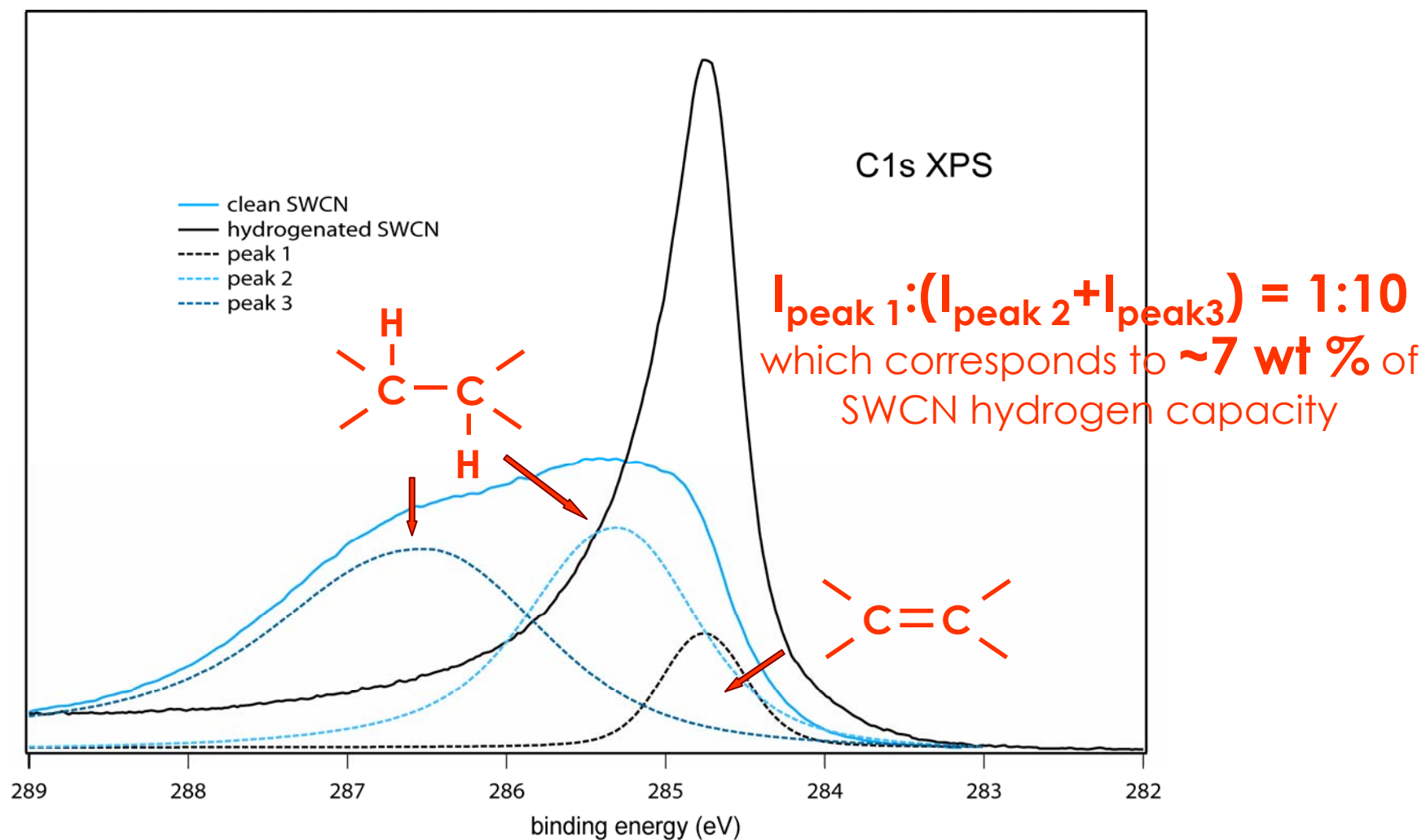
Calculated Values of the C1s shift due to the influence of the delocalized electron donated by adsorbed K atom

atom	shift, eV
C ₁	-0.483
C ₂	-0.403
C ₃	-0.372
C ₄	-0.739



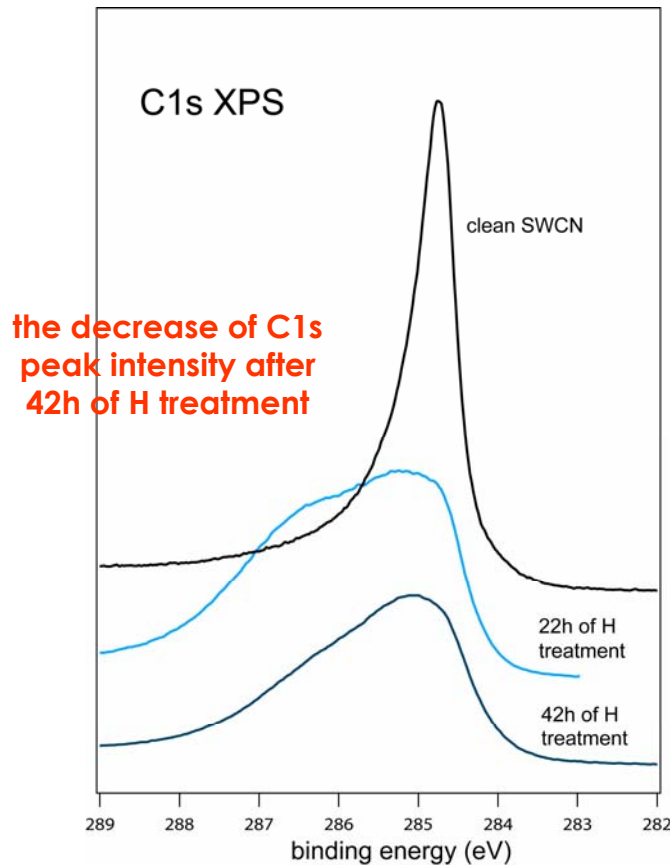
The hydrogenation degree of SWCN

Decomposition of C1s XPS for hydrogenated SWCN film

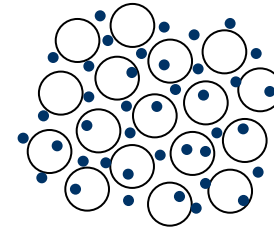


The interaction of atomic H with SWCN

Hydrogenation sequence of SWCN, type 1

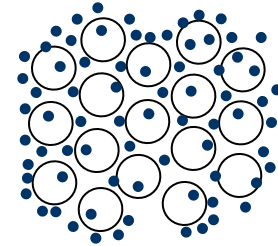


1. uniform hydrogenation of SWCN bundle up to 50 - 60 at %



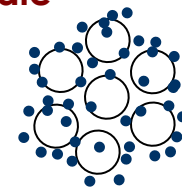
more atomic H

2. almost 100 at % hydrogenation of outer SWCN in the bundle



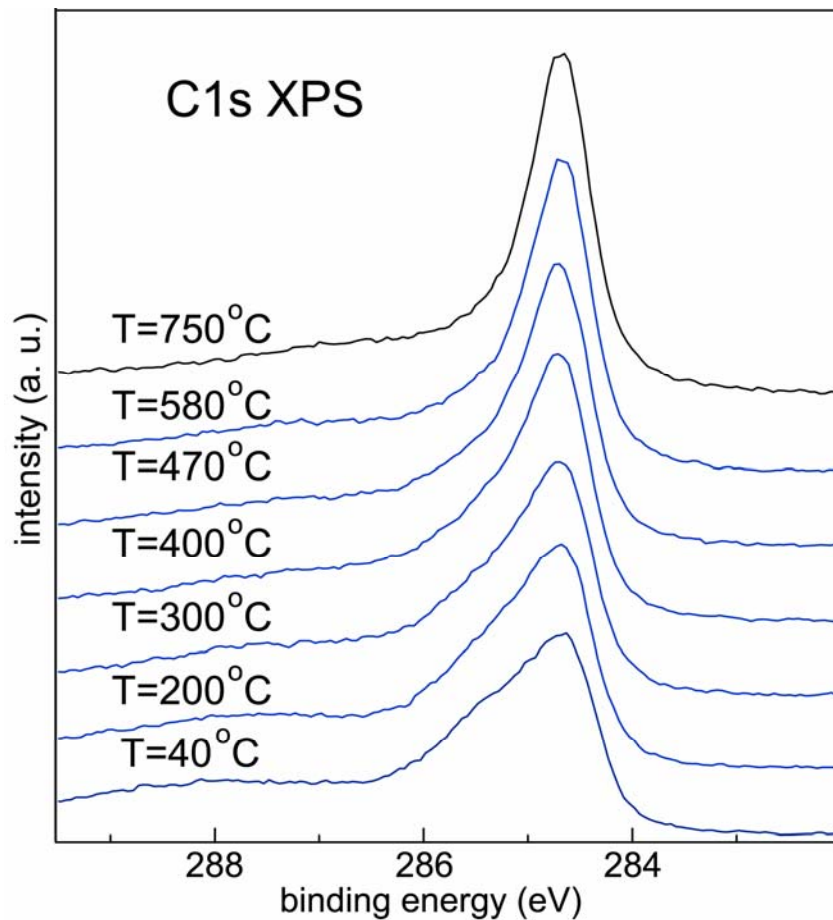
more atomic H

3. etching of outer 100% hydrogenated SWCN in the bundle



Hydrogen desorption temperature

C1s XPS spectra measured during annealing of H treated SWCN, type 1

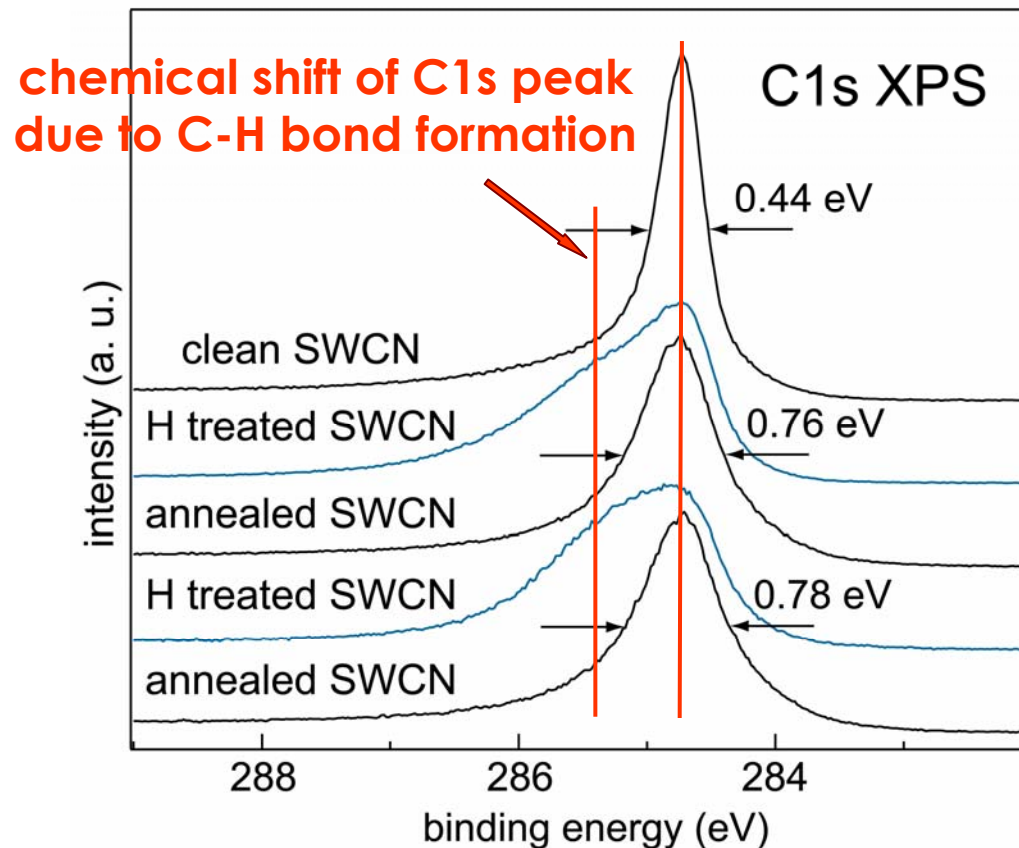


C1s peak shape change
due to C-H bond
cleavage was observed

Hydrogen desorption is observed in the range from **300 °C** to **600 °C**

Hydrogenation cycling

C1s XPS spectra of SWCN, type 1 exposed to two cycles of hydrogenation / dehydrogenation



Hydrogenation of SWCN film can be **cycled**

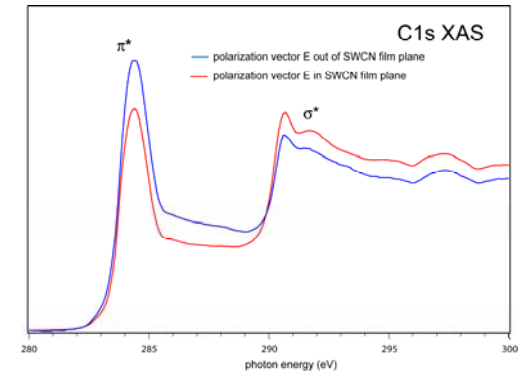
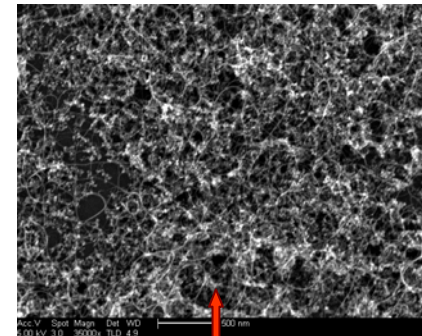
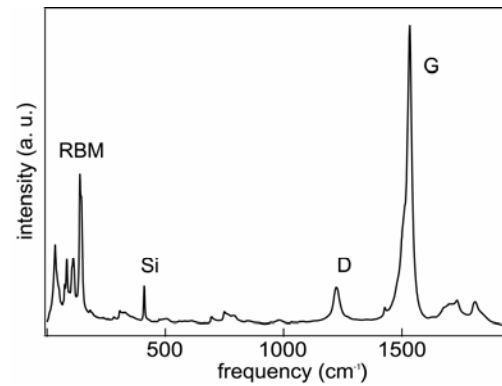
Hydrogenation cycling

Raman spectra

SEM picture

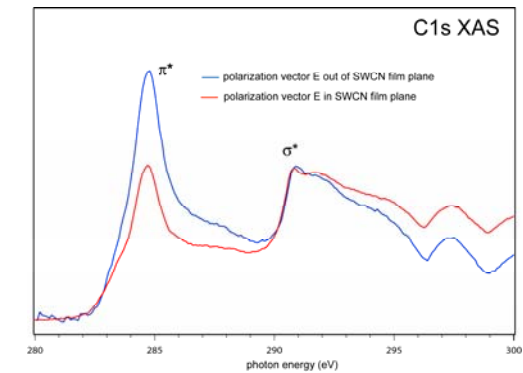
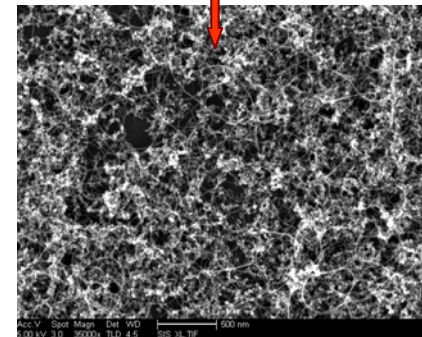
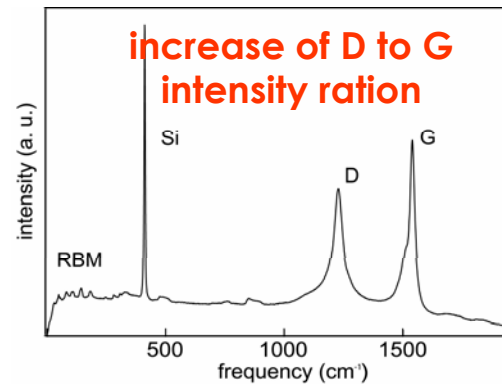
XAS spectra

Clean SWCN film



same morphology

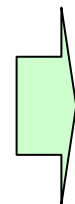
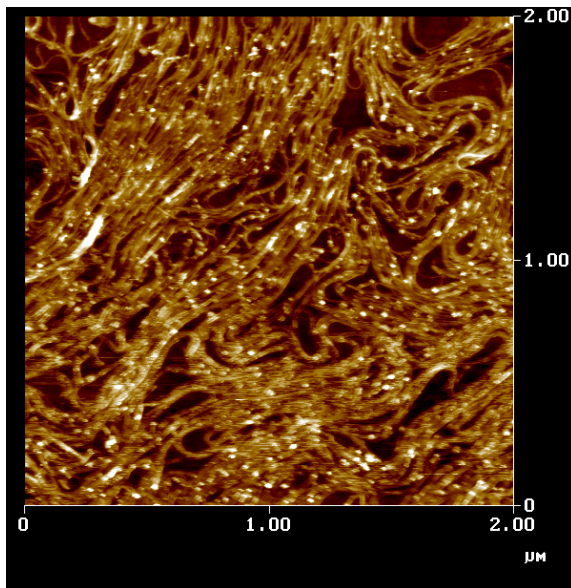
SWCN film exposed
hydrogenation /
dehydrogenation
cycle



Hydrogenation leads to the increase of the defect number in SWCN

Refining H-SWCN interaction

- to exclude the SWCN bundle influence on the observed results and to figure out the diameter range of SWCN which are stable at high degree of hydrogenation

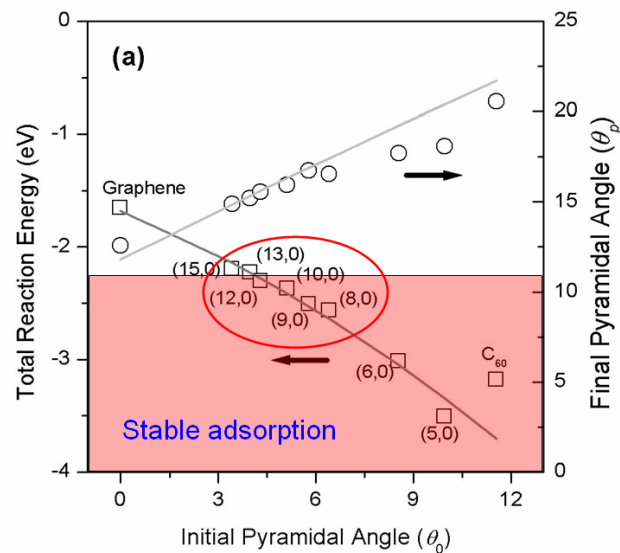


Step 1: to perform XAS and XPS spectroscopic study of H interaction with SWCN material using SWCN monolayers with known diameter distribution using AFM

The AFM image of SWCN monolayer prepared by Langmuir - Blodgett technique

Control of thermodynamics

- **technologically acceptable temperature range of H release is from 70 °C to 120 °C.**



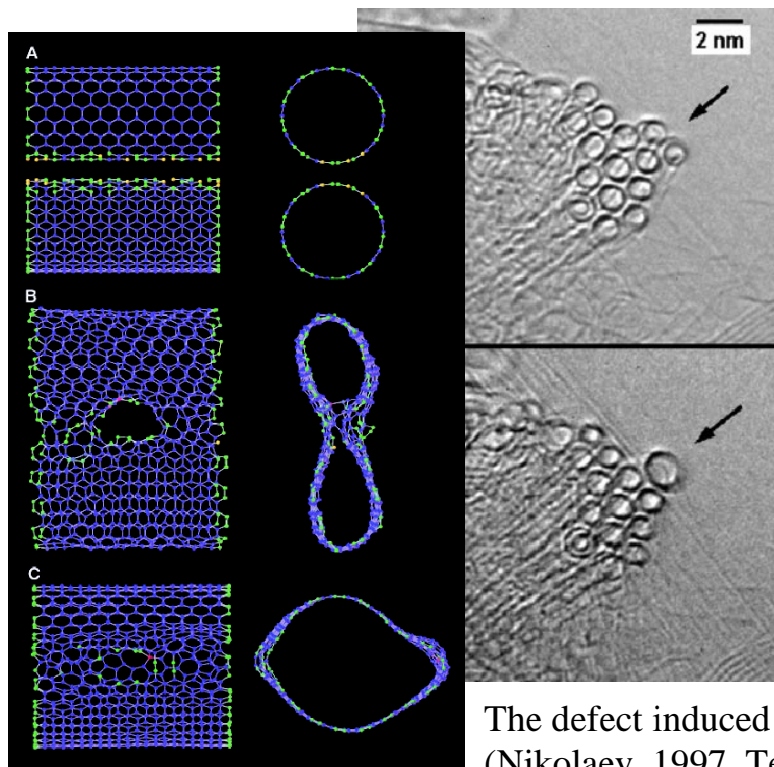
Step 2: to perform TP XPS measurements of fully hydrogenate SWCN films with two different diameter distribution.

Activation barrier?

Dependence of the C-H bond energy on the size of the SWCN according to the numerical modeling (KJ Cho, 2003).

Structural changes

- the role of defects in the SWCN hydrogenation process
- nanotube coalescence due to induced defects
- presence of CH_2 groups in hydrogenated SWCN

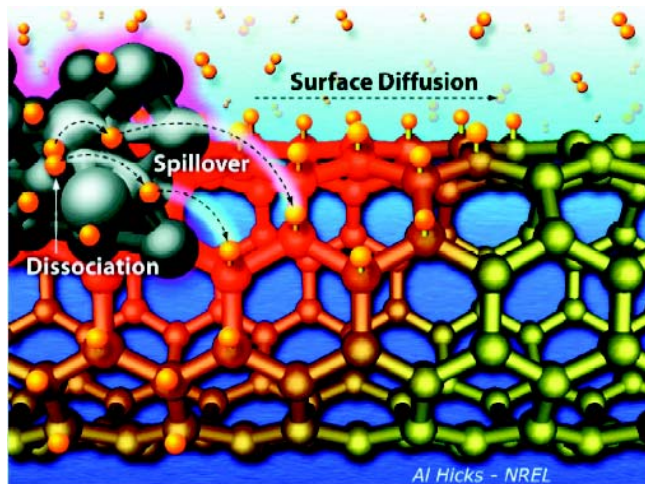


Step 3: to study SWCN material during several cycles of hydrogenation/ dehydrogenation using IR and Raman spectroscopies and STM

The defect induced coalescence of SWCN
(Nikolaev, 1997, Terrones, 2000)

Dissociation of molecular hydrogen

- hydrogenation of SWCN with molecular hydrogen



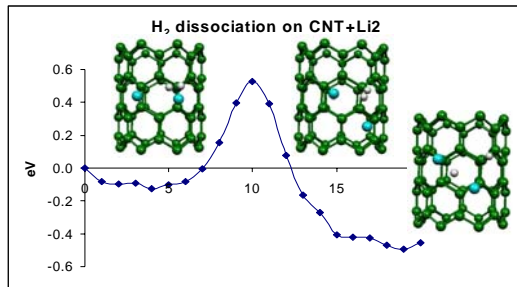
Hydrogenation via spillover mechanism (A.Lueking , 2002, A.Lueking , 2004)

Step 4: to study *in-situ* the interaction of SWCN with metals (Pt, Pd, Ni etc) capable to catalytically split H₂

Step 5: to study interaction of H₂ with SWCN - metal complexes.

Increased capacity

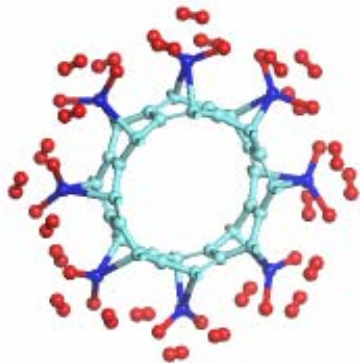
- chemisorption of hydrogen in Li-SWCN network



Step 6: to perform spectroscopic study of H interaction with SWCN with intercalated Li

- binding energy of H 0.457 eV
- dissociation barrier for H₂ around 0.529 eV

- molecular hydrogen adsorption on Ti-SWCN complex



Step 7: to perform spectroscopic study of H₂ interaction with Ti-SWCN complexes

Theoretical model of C₄TiH₈ with 7.7 wt% of H storage capacity (T. Yildirim, 2005)

Conclusions

- SWCN with different diameters can reach different hydrogenation degree before "unzipping" and etching
- for specific SWCN it is possible to hydrogenate **almost 100 at %** of the carbon atoms in the walls to form C-H bonds which corresponds to **7.7 weight %** of hydrogen capacity
- the hydrogenated SWNT are stable from ambient temperature to **300 °C**
- hydrogenation/dehydrogenation process can be **cycled**.